

Transition from one- to two-dimensional island growth on metal (110) surfaces induced by anisotropic corner rounding

Yinggang Li*

Department of Chemistry, and Ames Laboratory, Iowa State University, Ames, Iowa 50011

M. C. Bartelt†

IPRT, and Ames Laboratory, Iowa State University, Ames, Iowa 50011

J. W. Evans

Department of Mathematics, and Ames Laboratory, Iowa State University, Ames, Iowa 50011

N. Waelchli, E. Kampshoff, and K. Kern

Institut de Physique Expérimentale, EPF Lausanne, CH-1015 Lausanne, Switzerland

(Received 7 August 1997)

We propose a kinetic model to describe the temperature dependence of the shape of islands formed during submonolayer epitaxy on anisotropic metal surfaces. Our model reveals that “anisotropic corner rounding” is the key atomic process responsible for a transition in island shape, from chain structures at lower temperatures, to compact islands at higher temperatures. Exploiting data for the temperature and flux scaling of the island density, we analyze such behavior observed experimentally in Cu/Pd(110) epitaxy, estimating activation barriers of 0.45 and 0.3 eV for anisotropic terrace diffusion, and 0.65 eV for the slow corner-rounding process. [S0163-1829(97)02344-8]

I. INTRODUCTION

Diffusion-mediated formation of islands or aggregates can produce a rich variety of manifestly far-from-equilibrium structures.¹ Such structures occur when processes leading to the restructuring or shape equilibration of growing islands are inefficient on the time scale of aggregation. Often, the relative time scales can in fact be controlled by variation of growth conditions. This in turn can lead to variation in island structure, e.g., from Witten-Sander fractal aggregates with monoatomic arm widths² for insignificant restructuring, to fractal or dendritic aggregates with thicker arms or to compact nonequilibrium growth shapes³⁻⁷ for partial restructuring, to quasiequilibrium shapes for efficient restructuring. Detailed analysis of such transitions in structure can provide information on the kinetically limited restructuring processes, and on the associated activation barriers, thus facilitating control of island structure.

This full range of behavior is seen in the formation of two-dimensional islands during submonolayer metal-on-metal epitaxy, where structure can vary dramatically with deposition conditions (flux and substrate temperature).³⁻⁸ An additional factor here is substrate symmetry, the growth process being potentially more complicated when the substrate is geometrically anisotropic as, e.g., with metal(110) or reconstructed metal(100) surfaces. Often elongated islands,^{9,10} and sometimes even linear chains,^{5,8} are observed. A basic question here is how substrate anisotropy influences the island structure. In semiconductor epitaxy of Si/Si(100), island elongation was found to be *perpendicular* to the direction of fast diffusion, and to be reduced for higher temperatures.¹¹ These features have been interpreted as resulting from an-

isotropy in incorporation at the two distinct types of island edges, involving transport via an evaporation-condensation mechanism.^{11,12} Other interpretations exist,¹³ but the shape anisotropy is invariably driven by an anisotropy in bonding. On metal surfaces, the island elongation is typically found to be *parallel* to the presumed direction of fast diffusion. This leads to the natural suggestion, for such systems as Cu/Pd(110),^{5,8} that the observed anisotropy in island shape may be related to the anisotropy in terrace diffusion.¹⁴ However, detailed analysis is currently lacking.

Consequently, in this paper, we consider the behavior of a simple model for submonolayer epitaxial growth on anisotropic metal surfaces. This model predicts a transition from roughly isotropic islands at “very low” temperature (T) to one-dimensional (1D) linear island structures at “moderate” T . This corresponds to the onset of one-way corner rounding of atoms diffusing at or near the island edges. A further transition from linear to two-dimensional island growth at higher T corresponds to the onset of two-way corner rounding. The model is then applied to provide a characterization of previously observed Cu island growth on Pd(110),^{5,8} at least up to the transition temperature for two-way corner rounding. Exploiting new experimental data for the flux scaling of the island density, we conclude that while terrace diffusion is indeed anisotropic in this system, the kinetic mechanism responsible for the occurrence of the island-shape transition is “anisotropic corner rounding.” This derives from anisotropic bonding at island edges, as suggested for the Si/Si(100) system, although the kinetic pathway for mass transport between island edges is likely different for Cu/Pd(110).

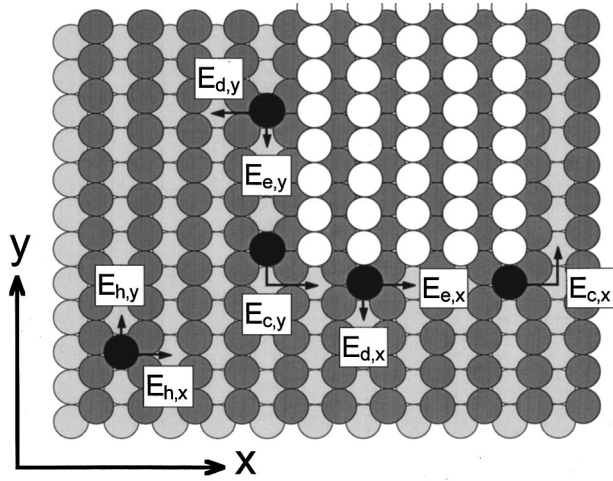


FIG. 1. Schematic of the metal (110) surface. Key atomistic processes and the notation for activation energies are shown.

II. MODEL FOR EPITAXIAL GROWTH ON FCC(110) SUBSTRATES

Several key atomistic processes for nucleation and growth of islands on fcc (110) substrates are indicated schematically in Fig. 1. These include (1) terrace diffusion of isolated adatoms with activation barriers $E_{h,x}$ and $E_{h,y}$ for hops along the x and y directions, respectively. Here $E_{h,x} > E_{h,y}$ since diffusion along the troughs of the fcc(110) surface is presumably easier than across them; (2) diffusion of edge atoms, with barriers $E_{e,x}$ and $E_{e,y}$ for hopping along the x and y edges, respectively; (3) two-step movement of edge atoms around island corners, with *effective* barriers $E_{c,x}$ and $E_{c,y}$ for transport from x to y edges, and y to x edges, respectively; and (4) detachment of edge atoms from the x and y edges with barriers $E_{d,x}$ and $E_{d,y}$, respectively. Kinetic rates for all the above processes will be obtained from an Arrhenius form, assuming a common attempt frequency of $\nu = 10^{12}/\text{s}$. The other key process not shown in Fig. 1 is (5) random deposition of atoms at rate F per empty site (measured in monolayers per second, ML/s). Deposition of adatoms on top of islands is not significant in the regime of low coverage ($\theta \leq 0.1$ ML) of interest here.

Some key relationships between the above activation barriers are expected to be satisfied in metal (110) systems. Let us assume significant interactions exist only between adatoms at adjacent adsorption sites. Specifically, let $E_{b,x}$ and $E_{b,y}$ denote the binding energies of an edge atom at x and y edges, respectively. On an fcc (110) surface, adjacent adatoms are nearest neighbors along a trough (the y direction), but are second-nearest neighbors across the trough, so we expect that $E_{b,y} \ll E_{b,x}$. Furthermore, let us first assume that the terrace diffusion barriers $E_{h,x}$ and $E_{h,y}$ apply for all sites not adjacent to the island (including the corner sites). Then, for corner rounding from the x to the y edge, the barrier for the first step is $E_{h,x} + E_{b,x}$ (as determined by detailed balance), and for the second step is $E_{h,y}$. Thus, the much larger barrier for the first “difficult” step determines $E_{c,x} = E_{h,x} + E_{b,x}$. For corner rounding in the reverse direction, there is a barrier for the first step of $E_{h,y} + E_{b,y}$, and for the second step of $E_{h,x}$, the latter being larger. After the first step, the atom can hop back with barrier $E_{h,y}$, so the corner sites have

a population $\rho_c \sim \exp[-E_{b,y}/(k_B T)]$ relative to that of the “initial” site occupied before the first hop. The effective rate for corner rounding is given by $\rho_c h_x$, and the effective barrier is $E_{c,x} = E_{h,x} + E_{b,x}$.¹⁵ Detailed balance also requires that $E_{d,x} = E_{h,y} + E_{b,x}$ and $E_{d,y} = E_{h,x} + E_{b,y}$. Using reasonable choices for Cu/Pd(110) of $E_{h,x} \approx 0.45$ eV, $E_{h,y} \approx 0.3$ eV, $E_{b,x} \approx 0.2$ eV, and $E_{b,y} \approx 0$ eV (see below), one finds that $E_{c,x} \approx 0.65$ eV, $E_{d,x} \approx 0.5$ eV, and $E_{c,y} \approx E_{d,y} \approx 0.45$ eV.

Next, we note that even interactions nominally only between adjacent adatoms can lower the activation barriers, e.g., for adatom hops between the corner and edge sites. This has important consequences for edge diffusion, and thus for island shape determination, as will become clear. The key observation is that $E_{c,x}$ could be significantly *reduced below* $E_{h,x} + E_{b,x}$ (and $E_{c,y}$ reduced below $E_{h,x} + E_{b,y}$), enhancing corner rounding of atoms diffusing at the island edge. Similarly, $E_{d,x}$ and $E_{d,y}$ could be reduced, although this turns out not to significantly affect island structure. Of course, if any barrier is reduced, then that for the reverse process must also be reduced to maintain detailed balance.

The above observations are critical for analysis of mass transport *between* island edges, which is the key process controlling island shapes. There are two competing kinetic pathways for this mass transport: edge or perimeter diffusion (PD), and 2D evaporation/recondensation, also called terrace diffusion (TD).¹⁶ For PD, the effective barriers for transport from x to y edges, and y to x edges, are $E_{c,x}$ and $E_{c,y}$, respectively. The inequality $E_{c,x} > E_{c,y}$ implies a strong direction-dependent efficiency for transport via PD. For TD, we emphasize that the corresponding effective barriers are generally *not* given by $E_{d,x}$ and $E_{d,y}$. Consider adatom evaporation from the x edge. This produces a quasiequilibrium density, $\rho_g \sim \exp[-E_{b,x}/(k_B T)]$, of adatoms near the x edge, relative to the density of edge atoms. Such evaporated atoms must hop “laterally” in the x direction with rate $h_x = \nu \exp[-E_{h,x}/(k_B T)]$ to reach a channel adjacent to the y edge of the island, thereafter allowing (easy) diffusion to and recondensation on the y edge. Thus, the effective rate for corner rounding from x to y edges via TD scales like $\rho_g h_x$, and the effective barrier is $E_{h,x} + E_{b,x}$, rather than the much lower value of $E_{d,x}$. Thus, one can see the importance of the above-mentioned possible significant reduction of $E_{c,x}$ below $E_{h,x} + E_{b,x}$, as this would enhance the PD over the TD pathway. Similar considerations show that the effective barrier for corner rounding from y to x edges via TD is $E_{h,x} + E_{b,y}$, so again PD can dominate if $E_{c,y}$ is significantly reduced below $E_{h,x}$. In any case, there is clearly a strong direction-dependent efficiency for transport via TD, just as for PD, which is driven by the anisotropy in bonding.

Based on the above picture of metal (110) epitaxy, we now discuss the qualitative behavior expected for the average island density N_A (number of islands per unit area), and the average linear island density, N_L (number of islands per unit length in the x direction across the troughs). These can be independently measured experimentally,⁸ but they are related by $N_L = \langle L \rangle N_A$, where $\langle L \rangle$ is the average length of islands (in the y direction). We also examine the average aspect ratio, $\alpha = \langle L/W \rangle$, where L and W give the length and width of islands, in the y and x direction, respectively. Note

that the mean island size satisfies $S_{av} = \theta/N_A \approx \langle L \rangle \langle W \rangle$, so $N_L = \langle L \rangle N_A \approx \theta / \langle W \rangle$.

The behavior of N_A is understood from conventional nucleation theory,¹⁷ which involves the concept of an effective critical size, i , above which islands are stable. For ‘‘low’’ T , where island formation is irreversible ($i = 1$), N_A decreases monotonically with increasing T , i.e., with increasing terrace diffusion rates. Its Arrhenius slope is determined by the terrace diffusion barriers, and depends on the degree of diffusional anisotropy.¹⁸ For higher T , where island formation becomes reversible, and $i > 1$, the Arrhenius slope of N_A increases, and also depends upon adatom bonding. An increase in i also influences the flux scaling of N_A . Behavior of N_L is more complex, and is naturally characterized by three regimes.

Regime I occurs for ‘‘low’’ T only if corner rounding is inoperative in *either* direction, but if there is significant terrace diffusion at least in the y direction (which requires that $E_{c,y} > E_{h,y}$). The resulting islands are roughly isotropic ($\alpha \approx 1$), even if terrace diffusion is anisotropic, and tend to be irregular or fractal. At fixed θ , N_L decreases with increasing T , as does N_A .

Regime II occurs for temperatures where terrace diffusion is significant, and anisotropic (one-way) corner rounding occurs, edge atoms being transported from the y to the x edge, but not in the reverse direction. Consequently, islands become elongated along the y direction, and $\langle L \rangle$ increases rapidly. This can result in an initial slight increase of $N_L = \langle L \rangle N_A$ with increasing T , even though N_A decreases. Eventually, transport from the y edge becomes so efficient that the islands become chainlike with near-constant width $W^{(II)} \approx 1 - 2$ atoms. Thus $N_L = \langle L \rangle N_A \approx \theta / W^{(II)}$ is independent of T , and α increases with increasing T like $1/N_A$.

In regime III, as T is increased even further, two-way corner rounding occurs. Transport from x to y edges competes increasingly with that from y to x edges, so islands become two-dimensional, and $N_L = \theta / \langle W \rangle$ and α decrease. At the onset of this regime or soon after, one also expects a transition to reversible island growth, so the Arrhenius behavior of N_L (and α) is further complicated, and contains information about adatom bonding.

It is appropriate to compare the above shape evolution with the equilibrium island shapes, which are also anisotropic for systems with anisotropic bonding. Clearly, in regime I, the shapes are far from equilibrium. This is also true in Regime II. Here one-way corner rounding produces a kinetic shape anisotropy, contrasting true equilibration (which requires all processes be two way). In regime III, shapes become closer to equilibrium for which anisotropy decreases with increasing T .

III. APPLICATION TO EPITAXIAL GROWTH OF Cu ON Pd(110)

As an application, we consider submonolayer epitaxy of Cu on Pd(110), where N_A , N_L , and α have been measured as a function of T , between 180 and 420 K (for fixed $F \approx 10^{-3}$ ML/s and $\theta \approx 0.1$ ML).^{5,8} The key observations were (a) an Arrhenius slope for N_A of $E = 0.12 \pm 0.01$ eV, for T above 200 K, with a break in this slope around 325 ± 20 K; (b) constant N_L for $T < T_c = 265 \pm 15$ K, decreasing thereaf-

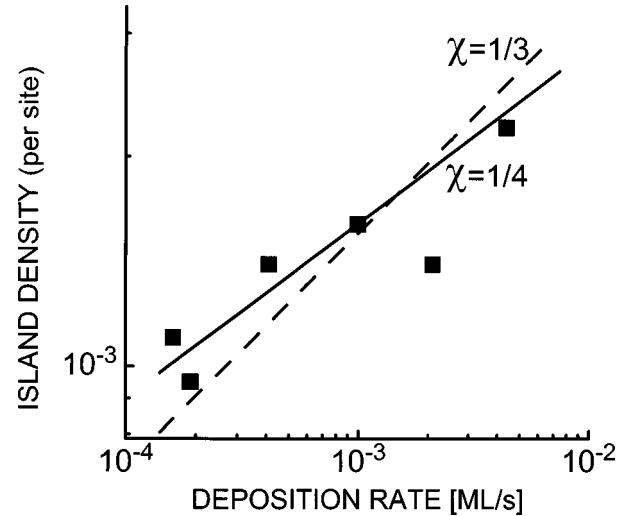


FIG. 2. Island density N_A vs flux F at 280 K. Experimental data are denoted by symbols. The ‘‘fit’’ with a solid (dashed) line corresponds to an exponent of $\chi = 1/4$ ($\chi = 1/3$).

ter; (c) a transition from 1D to 2D island growth with T increasing above T_c as reflected in the behavior of the aspect ratio. One plausible explanation of this behavior suggested in Refs. 5 and 8 was that terrace diffusion is basically one-dimensional (constrained along the troughs) when $T < T_c$, and that the activation of diffusion across the troughs for $T \geq T_c$ induces the 1D to 2D island shape transition (as well as a decrease in N_L , and a change in the Arrhenius slope of N_A). This scenario leads to estimates of $E_{h,y} \approx 4E \approx 0.5$ eV (cf. Ref. 18) from the Arrhenius behavior of N_A , and of $E_{h,x} \approx 0.75$ eV from the presumed onset of cross-trough diffusion at $T \approx T_c$.^{5,8}

In fact, direct experimental assessment of the nature of diffusion can be provided by analysis of the scaling of $N_A \sim F^\chi$, with deposition flux F (at fixed T and coverage). At lower T , where island formation is irreversible, and provided diffusion of small clusters is not significant, one has¹⁸ $\chi \approx 1/3$ ($1/4$) if diffusion is isotropic (strongly anisotropic). See also Ref. 10. Consequently, we have performed experiments to determine this scaling for Cu/Pd(110). As with previous studies, experiments were performed in a multipurpose UHV chamber (base pressure 1×10^{-10} mbar) with a variable-temperature beetle-type STM. More details concerning the Pd(110) sample preparation, the Cu deposition procedure, and the STM imaging conditions are given in Refs. 5 and 8. These studies reveal a scaling exponent of $\chi \approx 0.2 - 0.28$, for $F = 0.2 - 4 \times 10^{-3}$ ML/s at 280 K (see Fig. 2), indicative of anisotropic rather than isotropic diffusion.

A more precise analysis of the behavior in the Cu/Pd(110) system, and determination of key parameters, is achieved by comparison with simulation results. Such studies also demonstrate that anisotropy in terrace diffusion is *not* sufficient (nor necessary) to produce island shape transitions of the type observed during Cu/Pd(110) epitaxy. Instead, *anisotropic corner rounding* controls this transition. Below, we compare the experimental observations with results from simulations for three distinct parameter choices, denoted models I–III. Model I incorporates strongly anisotropic diffusion based on the original interpretation of Refs. 5 and 8; for contrast, model II incorporates isotropic terrace diffusion;

model III constitutes our best fit to experiment.

The following key observations are useful in assessing behavior for different parameter choices. Firstly, in regime II (or I) of lower T , where corner rounding is one-way (or completely absent), there is effectively irreversible capture of aggregating atoms to the strongly bonded x edge. Thus simplified simulations with irreversible capture (critical size $i = 1$) can be used to analyze this regime. The island density is controlled by the terrace diffusion barriers, and satisfies well-known scaling laws for $i = 1$. Secondly, from simulations, one readily finds that T_c is controlled not by the anisotropy in terrace diffusion, but rather by the anisotropy in corner rounding. The following simple argument indicates the dependence of T_c on model parameters, assuming corner rounding is dominated by PD. Suppose that transport from y to x edges is very efficient, so there is ample time for all adatoms aggregating with an island to be incorporated at the x edge during growth. Then, compare this incorporation rate (corresponding to the impingement rate, $I \approx F/N_A$, of adatoms onto islands) with the reverse transport rate for corner crossing, $h_{c,x}$, from x to y edges. If $h_{c,x} \ll I$, then adatoms impinging on the island are incorporated at the narrow x edges before they have a chance to move to or back to the y edge. Thus chainlike islands grow parallel to the y axis. At T_c , one should have $h_{c,x} \approx I$, which implies that $T_c \approx E_{c,x} / [k_B \ln(\nu N_A / F)]$.

First, we report the results of our analysis of behavior for lower T where it suffices to use simulations of simplified models with $i = 1$. Model I sets $E_{h,x} = 0.75$ eV and $E_{h,y} = 0.51$ eV, thus matching the Arrhenius slope $E \approx E_{h,y}/4$ of N_A .¹⁸ However, the actual values of N_A are far above the observed values, and correspondingly the α values are far too small. Reasonable choices of $E_{b,x} = 0.15$ – 0.3 eV introduce anisotropic corner rounding and an island shape transition, but with a too high value for T_c . Model II purposely incorporates isotropic terrace diffusion to emphasize that anisotropy in terrace diffusion is not needed to produce the transition in island shapes. We choose $E_{h,x} = E_{h,y} \approx 3E \approx 0.4$ eV (cf. Refs. 17 and 18) to match the experimental Arrhenius data. With a reasonable choice for $E_{b,x}$, this model agrees with the actual experimental values and T dependence of N_A and α significantly better than model I. However, Model II has $\chi \approx 1/3$, thus failing to match our new experimental data for the flux dependence of N_A . Model III provides our best fit to all the experimental data. Here, we adjust parameters from model II values by introducing some anisotropy in terrace diffusion into the model to lower χ from $1/3$ towards $1/4$,¹⁸ while retaining our match of the values of N_A . This is achieved by lowering $E_{h,y}$ to 0.30 eV, and simultaneously raising $E_{h,x}$ to 0.45 eV.

Finally, we report more comprehensive simulation results for a *simplified version* of model III, where we *switch off* the detachment from x and y edges (so $E_{d,x} = E_{d,y} = \infty$), and treat as immobile all atoms with lateral coordination of two or higher. Thus, we bias the PD pathway over TD. This choice mimics the case where $E_{c,x}$ is reduced below $E_{h,x} + E_{b,x}$. Model behavior is not sensitive to the low choice of $E_{e,y}$, which is set equal to $E_{h,y}$, or to the choice of $E_{e,x}$ (provided it does not exceed $E_{c,x}$), which is set equal to $E_{c,x}$.¹⁹ To allow some reversibility into the model (and, thus, also some

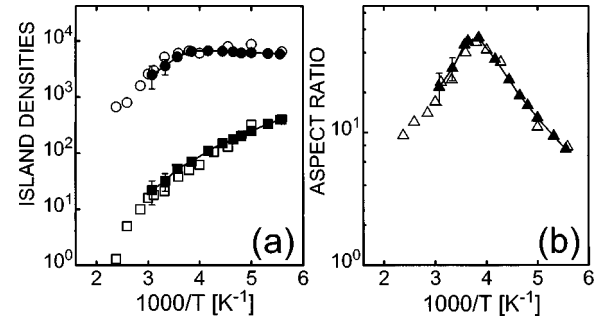


FIG. 3. Arrhenius behavior of N_L (circles), N_A (squares), and α (triangles). Open symbols are experiment data (Refs. 5 and 8). Solid symbols are simulation results (averaged over 20 runs) for model III, using the experimental values of $F \approx 10^{-3}$ ML/s and $\theta \approx 0.1$ ML. $N_A = 1$ ($N_L = 1$) corresponds to 1.7×10^{10} islands/cm² (420 islands/cm).

TD), we do allow atoms to escape from islands via diagonally adjacent sites while rounding corners. For consistency with the above, the barriers for such escape in the x (y) direction should exceed $E_{h,x}$ ($E_{h,y}$), but for simplicity are set equal to these values here. We caution that strictly this *violates* detailed balance, so quantitative predictions should be questioned above T_c . However, these details do not significantly affect model behavior in regime II of one-way corner rounding and effectively irreversible capture at x edges. We choose $E_{h,x} = 0.45$ eV and $E_{h,y} = 0.3$ eV, as indicated above, and set $E_{c,x} = 0.65$ eV based on the above formula for T_c , which equals 265 K here. Results shown in Figs. 3(a)–3(b) agree well with experiment. N_A has an Arrhenius slope of ~ 0.1 eV, when $T \approx 200$ – 325 K, for $F \approx 10^{-3}$ ML/s, and a χ of about 0.26, at 280 K, for $F \approx (0.2$ – $4) \times 10^{-3}$ ML/s. The simulations confirm that $\alpha \approx 0.6\theta/N_A$, for $T < T_c \approx 265$ K, corresponding to an average island width of 1.5 – 2 atoms, as in the experiment. Simulated island configurations for $T = 265$ – 320 K are similar to those in the STM images, as shown in Fig. 4. However, for higher T , the model is inadequate, and a fully reversible model, which precisely satisfies detailed balance, should be used.

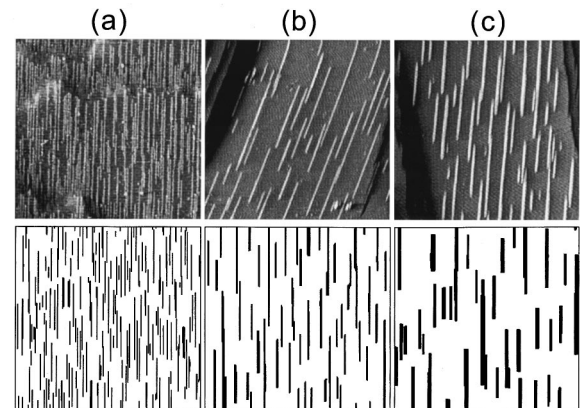


FIG. 4. Top row: STM images (Refs. 5 and 8) of Cu islands grown on Pd(110), at (a) 265 K, (b) 300 K, and (c) 320 K. Bottom row: corresponding simulated film morphologies using model III (with the experimental $\theta \approx 0.1$ ML and $F \approx 10^{-3}$ ML/s). Panels are $1200 \text{ \AA} \times 1200 \text{ \AA}$.

IV. SUMMARY

We have demonstrated the general importance of anisotropy in corner rounding for island shape transitions in epitaxy on anisotropic surfaces. Simulations, together with new data for flux scaling of the island density, reveal that while there is anisotropy in surface diffusion in submonolayer deposition of Cu on Pd(110), anisotropy in corner rounding is the key process producing the observed dramatic transition from 1D chainlike islands to 2D islands, with increasing T . We estimate activation barriers of $E_{h,x}=0.45$ eV and $E_{h,y}=0.3$ eV for anisotropic terrace diffusion, and of $E_{c,x}=0.65$ eV for the slow corner-rounding process. These results imply that $E_{b,x}\geq 0.2$ eV. Finally, we note that corner and kink rounding are also of importance for epitaxy on isotropic metal (111) surfaces. The detailed features of these

processes control the initial arm thickening and shape evolution of fractal or dendritic islands often observed at very low T ,²⁰ and kink rounding is crucial in quenching such shape instabilities at higher T .⁷ Thus, the details of edge transport and, specifically, of corner rounding, are of general importance in determining nonequilibrium island growth shapes during epitaxy.

ACKNOWLEDGMENTS

The theoretical work was supported by NSF grants CHE-9224884 (Y.L.), and CHE-9700592 (M.C.B. and J.W.E.). It was conducted at Ames Laboratory, which is operated for the U.S. DOE by Iowa State University under Contract No. W-7405-Eng-82. We would also like to acknowledge valuable discussions with Andrew DePristo.

*Present address: Ericsson Microwave Systems AB, UR, S-431 84 Molndal, Sweden.

†Present address: Sandia National Laboratories, MS 9161, Livermore, CA 94550.

¹H. E. Stanley and N. Ostrowsky, *On Growth and Form* (Kluwer, Boston, 1986).

²T. A. Witten and L. M. Sander, *Phys. Rev. Lett.* **47**, 1400 (1981).

³R. Q. Hwang, J. Schröder, C. Günther, and R. J. Behm, *Phys. Rev. Lett.* **67**, 3279 (1991).

⁴T. Michely, M. Hohage, M. Bott, and G. Comsa, *Phys. Rev. Lett.* **70**, 3943 (1993).

⁵H. Röder, E. Hahn, H. Brune, J.-P. Bucher, and K. Kern, *Nature (London)* **366**, 141 (1993).

⁶H. Brune, C. Romainczyk, H. Röder, and K. Kern, *Nature (London)* **369**, 469 (1994).

⁷M. C. Bartelt and J. W. Evans, *Surf. Sci. Lett.* **314**, L829 (1994); H. Röder, K. Bromann, H. Brune, and K. Kern, *Phys. Rev. Lett.* **74**, 3217 (1995).

⁸J.-P. Bucher, E. Hahn, P. Fernandez, C. Massobrio, and K. Kern, *Europhys. Lett.* **27**, 473 (1994); E. Hahn, E. Kampshoff, A. Fricke, J.-P. Bucher, and K. Kern, *Surf. Sci.* **319**, 277 (1994).

⁹S. Günther, E. Kopatzki, M. C. Bartelt, J. W. Evans, and R. J. Behm, *Phys. Rev. Lett.* **73**, 553 (1994).

¹⁰T. R. Linderoth, J. J. Mortensen, K. W. Jacobsen, E. Lægsgaard, I. Stensgaard, and F. Besenbacher, *Phys. Rev. Lett.* **77**, 87 (1996). This work suggests that the exponent of 1/4 found in Ref. 18 for a point-island model with 1D diffusion is shifted to 1/3 for islands of finite extent. This is not observed in our model, or in new benchmark studies of a square-island model [M. C. Bartelt and J. W. Evans (unpublished)].

¹¹Y.-W. Mo, J. Kleiner, M. B. Webb, and M. G. Lagally, *Phys. Rev. Lett.* **66**, 1998 (1991); Y.-W. Mo, B. S. Swartzentruber, R.

Kariotis, M. B. Webb, and M. G. Lagally, *Phys. Rev. Lett.* **63**, 2393 (1989).

¹²V. M. Bedanov and D. N. Mukhin, *Surf. Sci.* **278**, 364 (1992); **297**, 127 (1993).

¹³Z. Zhang, Y.-T. Lu, and H. Metiu, *Surf. Sci. Lett.* **255**, L543 (1991); P. Kleban, *J. Vac. Sci. Technol. A* **10**, 2436 (1992).

¹⁴Our simulations of a simple model for the formation of compact islands via 1D diffusion do reveal shape anisotropy [M. C. Bartelt and J. W. Evans (unpublished)], contrasting Refs. 10 and 11.

¹⁵Note that if $E_{b,x} > E_{b,y}$ (as above), but now $E_{h,x} < E_{h,y}$, then one has $E_{c,x} = E_{h,y} + E_{b,x}$ and $E_{c,y} = E_{h,y} + E_{b,y}$.

¹⁶S. V. Khare, N. C. Bartelt, and T. L. Einstein, *Phys. Rev. Lett.* **75**, 2148 (1995); P. A. Thiel and J. W. Evans, in *Morphological Organization in Epitaxial Growth and Removal*, edited by Z. Zhang and M. G. Lagally (World Scientific, Singapore, 1997).

¹⁷J. A. Venables, *Philos. Mag.* **27**, 697 (1973); M. C. Bartelt, L. S. Perkins, and J. W. Evans, *Surf. Sci. Lett.* **344**, L1193 (1995). Stable in-trough dimers imply $i=1$ scaling at low T .

¹⁸M. C. Bartelt and J. W. Evans, *Phys. Rev. B* **46**, 12 675 (1992); *Europhys. Lett.* **21**, 99 (1993); J. Villain, A. Pimpinelli, L. Tang, and D. Wolf, *J. Phys. I* **2**, 2107 (1992).

¹⁹Corrected effective medium calculations [T. J. Raeker and A. E. DePristo, *Int. Rev. Phys. Chem.* **10**, 1 (1991)] suggest that barriers for edge diffusion are about 10% greater than for terrace diffusion. Edge diffusion barriers were observed to be lower than corner rounding barriers in metal(100) homoepitaxy [G. L. Kellogg, *Surf. Sci.* **359**, 237 (1996)], and we expect that $E_{e,x} < E_{c,x}$.

²⁰M. Hohage, M. Bott, M. Morgenstern, Z. Zhang, T. Michely, and G. Comsa, *Phys. Rev. Lett.* **76**, 2366 (1996); H. Brune, H. Holger, K. Bromann, K. Kern, J. Jacobsen, P. Stoltze, K. Jacobsen, and J. Nørskov, *Surf. Sci. Lett.* **349**, L115 (1996).